Atmos. Chem. Phys. Discuss., https://doi.org/10.5194/acp-2018-77
Manuscript under review for journal Atmos. Chem. Phys.
Discussion started: 15 February 2018

Atmospheric Chemistry and Physics Discussions

Low hygroscopicity of organic material in anthropogenic aerosols under pollution episode in China

Juan Hong[1,2,3,4], Hanbing Xu[5], Haobo Tan[6*], Changqing Yin[6], Liqing Hao[7], Fei Li[6], Mingfu Cai[8], Xuejiao Deng[6], Nan Wang[6], Hang Su[1,3], Yafang Cheng[1,3], Lin Wang[4*], Tuukka Petäjä[2], Veli-Matti Kerminen[2]

[1]Institute for Environmental and Climate Research, Jinan University, Guangzhou, Guangdong 511443, China
[2]Department of Physics, University of Helsinki, P.O. Box 64, Helsinki 00014, Finland
[3]Multiphase Chemistry Department, Max Planck Institute for Chemistry, Mainz 55128, Germany
[4]Shanghai Key Laboratory of Atmospheric Particle Pollution and Prevention, Department of Environmental Science & Engineering, Fudan University, 220 Handan Road, Shanghai 200433, China
[5]Experimental Teaching Center, Sun Yat-Sen University, Guangzhou 510275, China
[6]Institute of Tropical and Marine Meteorology/Guangdong Provincial Key Laboratory of Regional Numerical Weather Prediction, CMA, Guangzhou 510640, China
[7]Department of Applied Physics, University of Eastern Finland, Kuopio 70211, Finland
[8]School of Atmospheric Sciences, Guangdong Province Key Laboratory for Climate Change and Natural Disaster Studies, and Institute of Earth Climate and Environment System, Sun Yat-sen University, Guangzhou, Guangdong 510275, China

Correspondence to: Haobo Tan (hbtan@grmc.gov.cn) and Lin Wang (lin_wang@fudan.edu.cn)

Abstract

Simultaneous measurements of aerosol hygroscopicity and particle phase chemical composition were performed at a suburban site over the Pearl River Delta Region in the late summer of 2016 using a self-assembled Hygroscopicity Tandem Differential Mobility Analyzer (HTDMA) and an Aerodyne Quadruple Aerosol Chemical Speciation Monitor (ACSM), respectively. Hygroscopic growth factor (HGF) of Aitken (30 nm, 60 nm) and accumulation mode (100 nm, 145 nm) particles was obtained under 90% relative humidity (RH). An external mixture was observed for all-sized particles during this study, with a dominant mode of more hygroscopic (MH) particles as aged aerosols dominated due to the anthropogenic influence. The HGF of less hygroscopic (LH) mode particles increased, while their number fractions decreased, during the daytime due to a reduced degree of external mixing probably from the condensation of gaseous species. These LH mode particles in the early morning or late afternoon could be possibly dominated by carbonaceous material emitted from local automobile exhaust during the rush hours. During polluted days with air masses mainly from the coastal areas, the chemical composition of aerosols had a clear diurnal variation and a strong correlation with the mean HGF. Closure analysis was carried out between the HTDMA-measured HGF and the ACSM-derived hygroscopicity using various approximations for hygroscopic growth factor of organic compounds (HGF_{org}). The result with HGF_{org} of below 1.1 suggests that the organic material in the aerosol from this suburban site, which represents a more anthropogenically influenced aerosol, is close to being

hydrophobic even under 90% RH. According to the closure analysis, a simple linear relationship between HGF_{org} and the oxidation level inferred from the O:C ratio of the organic material was suggested for the current type of aerosols during this study. Compared with the results from other environments, HGF_{org} obtained from our measurements appeared to be less sensitive to the variation of its oxidation level. This finding suggests it is important to consider the differences in the relationship between HGF_{org} and the O:C atomic ratio observed in different laboratory and field environments. Moreover, this result provides an improved hygroscopicity parameterization of organic material in anthropogenically influenced aerosols that can be incorporated into large-scale modeling frameworks, especially for the suburban context in China.

1. Introduction

Aerosol hygroscopicity describes the interaction between aerosol particles and ambient water molecules at both sub and supersaturated conditions in the atmosphere. It is a key property to affect the size distribution of ambient aerosols and can indirectly give information on particle compositions (Swietlicki et al., 2008; Zhang et al., 2011). It also plays an important role in visibility degradation and multiphase chemistry due to an enlarged cross-section area of aerosol particles after taking up water in humid environment (Tang et al., 1996; Malm et al., 2003; Cheng et al., 2008; Liu et al., 2013; Li et al., 2014; Zheng et al., 2015; Cheng et al., 2016). Moreover, it determines the number concentration of cloud condensation nuclei and the lifetime of the clouds, which in turn affect the regional and global climate indirectly (Zhang et al., 2008; Reutter et al., 2009; Su et al., 2010; IPCC, 2013; Rosenfeld et al., 2014; Schmale et al., 2014; Seinfeld et al., 2016; Zieger et al., 2017).

Hygroscopicity measurements have been conducted in numerous laboratory and field conditions around the world. Different observational findings related to hygroscopic properties of particles and their chemical composition were obtained for aerosols from various environmental background conditions. (Bougiatioti et al., 2009; Park et al., 2009; Swietlicki et al., 2008; Asmi et al., 2010; Tritscher et al., 2011; Whitehead et al., 2014; Hong et al., 2015; Chen et al., 2017). Recent studies have specially focused on the hygroscopicity of organic material, as atmospheric aerosols normally contain a large number of organic species, which exhibit highly various water uptake abilities. Previous works have extensively examined and reported the hygroscopicity of the organic fraction in aerosols worldwide, including boreal forest, rural and urban background areas (Chang et al., 2010; Wu et al., 2013; Mei et al., 2013; Hong et al., 2015; Wu et al., 2016). They found that the oxidation level or the oxygenation state of the entire organics is the major factor drives the water uptake ability of the organic fraction in aerosols. However, knowledge on the hygroscopicity of organic material and its dependency on the oxidation level of organics in urban background areas under high aerosol mass loading conditions, for instance, in China, is limited.

Due to the fast development of industrialization and urbanization, China has experienced increasingly severe air pollution during the few past decades (Zheng et al., 2015; Wang et al., 2017). High loadings of atmospheric aerosols can reduce visibility and lead to adverse acute and chronic health effects due to penetration and deposition of submicron particles in the human respiratory system (Dockery et al., 1993; Cabada

et al., 2004; Tie et al., 2009). In order to better understand the chemical composition, sources and aging processes of atmospheric aerosols and in turn target the atmospheric pollution problems in China, measurements of atmospheric particles with various purposes have increased during the recent years. Hygroscopicity, which is vital for understanding its impact on the multiphase chemistry, regional visibility, air quality and climate (Cheng et al., 2008; Gunthe et al., 2011; Cheng et al., 2016), has also been implemented into extensive campaigns in densely populated areas, such as North China Plain (Massling et al., 2009; Liu et al., 2011) and the Yangtze River Delta (Ye et al., 2013). In the Pearl River Delta (RPD) region, a metropolis in southeastern China with high aerosol loadings and low visibility probably due to anthropogenic emissions, hygroscopicity measurements have also been initiated during the past few years (Tan et al., 2013; Jiang et al., 2016; Cai et al., 2017). These previous studies have mainly focused on the statistical analysis of the hygroscopic properties of PRD aerosols and tried to give possible explanations for their temporal variations. However, the relationship between the hygroscopic properties of aerosols in PRD region and the particle phase chemical composition have not yet been systematically constrained, especially the relation of hygroscopic properties of the organic fraction in the particles to its oxidation level. Particularly, a close look at the hygroscopicity and chemical composition of particles during high aerosol loadings is also scarce.

In this study, we measured the size-dependent hygroscopic properties and non-size-resolved chemical composition by a self-assembly Hygroscopicity Tandem Differential Mobility Analyzer (HTDMA) and an Aerodyne Quadruple Aerosol Chemical Speciation Monitor (ACSM) respectively in a suburban site in PRD region. We aim to find the link between the hygroscopicity of aerosols and their chemical composition, with a focus on identifying the hygroscopic properties of the organic material and their O:C dependency for these suburban aerosols. Hygroscopic properties and chemical composition of particles under high and low aerosol loadings were particularly analyzed separately.

2. Materials and methodology

2.1 Sampling site and air mass origins

The measurements were conducted from 12 September to 19 October 2016 at the CAWNET (Chinese Meteorological Administration Atmospheric Watch Network) station in Panyu, Southern China. The site is located at the top of Dazhengang Mountain, which is in the suburban area of the megacity, Guangzhou. A figure on the geographical location is available in Tan et al. (2013) and Jiang et al. (2016). A detailed description of the CAWNET station and the sampling inlet can be found in Tan et al. (2013) and Cai et al. (2017).

To investigate the relationship between atmospheric aerosol hygroscopicity and the transport paths or source regions of air masses, 72-hour back trajectories of air parcels arriving at CAWNET were calculated at 6-hour intervals using the Hybrid Single-Particle Lagrangian Integrated Trajectory (HYSPLIT) model for this study. The arrival height of the trajectories was chosen at the sampling site, which is 150 m above ground level. Trajectories with similar spatial distributions or patterns were grouped together

to generate clusters, representing their mean trajectories and the predominant air mass origins during the campaign.

2.2 Measurements and data analysis

A self-assembled HTDMA was deployed to measure the hygroscopic growth factor (HGF), mixing state as well as the particle number size distribution (10-1000 nm) of ambient aerosols during this study. A detailed characterization of the HTDMA system and its operating principles are available in Tan et al. (2013b). Briefly, ambient aerosols after passing through a PM_1 impactor inlet were first brought through a Nafion dryer (Model PD-70T- 24ss, Perma Pure Inc.) to be dried to RH lower than 10% and were subsequently charged by a neutralizer (Kr^{85}, TSI Inc.). These dry particles of four specific mobility diameters (D_0; 30, 60, 100 and 145 nm) were selected by the first Differential Mobility Analyzer (DMA1, Model 3081L, TSI Inc.) in the HTDMA system and then were introduced into a membrane permeation humidifier (Model PD-70T-24ss, Perma Pure Inc.) to reach 90% RH. With a second DMA (DMA2, Model 3081L, TSI Inc.) and a condensation particle counter (CPC, Model 3772, TSI Inc.), the growth factor distributions (GFDs) or the mobility diameter (D_P) of these conditioned particles at 90% RH and room temperature were measured. The hygroscopic growth factor (HGF, RH=90%) is then defined as:

$$HGF(90\%) = \frac{D_p(RH=90\%)}{D_0}. \quad (1)$$

In practice, growth factor probability density function (GF-PDF) was fitted from the measured GFDs with bimodal lognormal distributions using TDMAfit algorithm (Stolzenburg, 1988; Stolzenburg and McMurry, 2008). After obtaining GF-PDF, the ensemble average hygroscopic growth factor (HGF), number fractions of particles at each mode and the spread of each mode were calculated.

An Aerodyne Quadruple Aerosol Chemical Speciation Monitor (ACSM, Aerodyne Research Inc.) was employed to determine the non-refractory PM_1 chemical composition and O:C of submicron aerosol particles with a 50% collection efficiency during the experimental period (Ng et al., 2011). The 'Ambient-Improved' ratios of oxygen to carbon (O:C) were then estimated by their relationship to the mass fractions of m/z44 (f44) to the total organic mass (Canagaratna et al., 2015). The mass concentration of black carbon was measured by an Aethalometer using a $PM_{2.5}$ inlet (Hansen et al., 1982). Wu et al. (2009) compared the BC concentration in PM_1 and $PM_{2.5}$, respectively and found that BC aerosols mainly exist in the fine particles. Due to the limited literature data on BC size distributions in the PRD region, we used the simplified approach by Wu et al. (2009) of the BC concentration in aerosols with different size scales to estimate the BC concentration in PM_1 for this study. It is necessary to note that the chemical composition of PM_1 can be different from those of individual size bins, especially Aitken mode particles, but might be close to those of accumulation mode particles. In addition, complimentary measurements for ambient meteorological conditions (e.g. relative humidity, wind direction and wind speed), as well as the particulate matter ($PM_{2.5}$) mass concentration measurements were conducted concurrently during the experimental period.

Atmos. Chem. Phys. Discuss., https://doi.org/10.5194/acp-2018-77
Manuscript under review for journal Atmos. Chem. Phys.
Discussion started: 15 February 2018

Atmospheric Chemistry and Physics Discussions

2.3 Closure study

Ambient particles are mixtures of a vast number and variety of species. In order to estimate the averaged hygroscopicity of ambient particles, the Zdanovskii–Stokes–Robinson (ZSR) mixing rule (Zdanovskii, 1948; Stokes and Robinson, 1966) was assumed and the hygroscopic growth factor (HGF_m) of a mixed particle was calculated by summarizing the volume-weighted HGF of the major chemical components of aerosol particles:

$$\mathrm{HGF}_m = (\sum_i \varepsilon_i \cdot \mathrm{HGF}_i^3)^{1/3}, \quad (2)$$

where ε_i is the volume fraction of each species and HGF_i is the growth factor of each species present in the mixed particle. The volume fraction of each species was calculated from their individual dry densities and mass fractions from ACSM data (Gysel et al., 2007; Meyer et al., 2009) by neglecting the interactions between different species. Since ACSM measures the concentration of ions, the molecular composition can be reconstructed from the ion pairing based on the principles of aerosol neutralization and molecular thermodynamics (McMurry et al., 1983; Kortelainen et al., 2017). Several neutral molecules such as $(NH_4)_2SO_4$, NH_4HSO_4, NH_4NO_3, H_2SO_4 and other possible species were therefore obtained. The related properties of each species necessary for the calculation in Eq. 2 are listed in Table 1. An ensemble value of HGF_{org}=1.1 was used, as the best-fit values of the closure analysis was achieved, which is detailed in Sect. 3.4. As suggested in early studies, the hygroscopicity of organics in the aerosol particles is dependent on their degree of oxygenation inferred from the O:C ratio (Massoli et al., 2010; Duplissy et al., 2011; Hong et al., 2015), hence, we further estimated HGF_{org} according to the degree of oxygenation presented by the O:C ratio. A similar approach to approximate the hygroscopicity of organics in particle phase based on their O:C ratio is also proposed by Hong et al. (2015). A density value of 1250 kg/m^3 was used for the organics to calculate their volume fraction, which was suggested by Yeung et al. (2014) in their closure analysis for aerosols from a similar environment.

3. Results and Discussions

3.1 Overview of measurements

Figure 1 shows the temporal variations of meteorological conditions (e.g., relative humidity, wind direction, average wind speed) and $PM_{2.5}$ as well as BC mass concentration in PM_1. In general**,** RH showed a clear diurnal cycle and a northern wind was frequently experienced during this study. The range of particle mass concentration ($PM_{2.5}$) varied from 20 to 180 μg/m^3, with relatively low values (roughly below 50 μg/m^3) during most of the time. Previous $PM_{2.5}$ mass concentration measurements at this site have yielded quite similar results (Jiang et al., 2016) at this season. During the period of September 22 to 27, the PRD region experienced stagnant weather conditions, with low wind speeds and fluctuating wind directions near the surface. The stagnant weather leads to the observed increase in the mass concentrations of $PM_{2.5}$ and BC, with up to about two times higher values compared with the rest of this study.

Figure 2 shows an overview GF-PDF for particles of four different diameters colored with probability density and the mass fractions of the ACSM chemical components as

well as the particle number size distribution (10-1000 nm) over the entire measurement period. The white gap in the mass fraction data in the fifth panel is due to an instrument failure. Particles of all sizes showed apparent bimodal growth factor distributions with a mode of more hygroscopic particles and a mode of less hygroscopic particles, indicating the particle population was mainly externally mixed. A similar feature was also observed in the PRD region previously (Eichler et al., 2008; Tan et al., 2013b; Jiang et al., 2016; Cai et al., 2017), as well as in other urban environment around the world (Massling et al., 2005; Fors et al., 2011; Liu et al., 2011; Ye et al., 2013).

In our study, the bimodal distributions had a dominant more hygroscopic (MH) mode for larger particles (100 nm, 145 nm), whereas for smaller particles (30 nm, 60 nm) these number fraction of two modes were approximately of similar magnitude. From the fifth panel in Fig.1, we can see that inorganics were the dominant components of PM_1 at the PRD region, which is contrary to a boreal forest environment where organics dominated the aerosol composition (Hong et al., 2015). This is not a surprise due to the stronger anthropogenic influence in our measurement site. Particle number size distributions below 10 nm were not measured by our setup, so, new particle formation events could not be systematically classified for this study. However, a subsequent particle growth from 10 nm to the accumulation mode was periodically observed. In this study, two distinguished types of days (e.g., one as 'relative clean days' during September 12 to 19 and October 9 to 15 and one as 'polluted days' during September 22, 18:00 to September 27, 9:00) were characterized by their corresponding differences in meteorological conditions, the mass concentration of $PM_{2.5}$ or BC as well as the occurrence of clear particle growth above 10 nm. Distinct analysis of aerosol hygroscopicity, chemical composition as well as air mass origins for these two periods will be further discussed in Sect. 3.3.

3.2 Hygroscopicity and mixing state

Figure 3 shows the diurnal variations of the average HGF of particles of four different sizes. In general, larger particles were more hygroscopic than smaller particles. No strong diurnal pattern of the mean HGF can be concluded from the current results, after taking into account the uncertainties associated with the mean values. This suggests complex sources and aging processes of aerosols at this suburban site. In brief, HGFs of particles were the highest during the daytime, started to decrease at about 3:00 pm, and reached the minimum values at about 8:00 pm. The reduction of the mean HGF during the late afternoon can be explained by the influence of the higher contributions of traffic emissions during rush hours from afternoon until evening (Cheng et al., 2012). However, we did not observe the effect of the morning traffic, which will be further discussed in Sect. 3.3.

In the upper panels of Fig. 4, we compared the diurnal variation of the HGFs of particles in the LH and MH mode. HGFs of LH mode of particles of all sizes started to increase after 10:00 am and decrease at about 3:00 pm until reaching their lowest levels at about 8:00 pm. A possible candidate for these LH mode particles could be carbonaceous material emitted from local automobile exhaust during the rush hours, with black carbon or soot and water-insoluble organics as the major components. These freshly less hygroscopic particles started to age in the atmosphere by condensation of different vapors or multiphase reactions in the daytime, leading to an obvious increase in HGFs

of LH mode particles without reaching that of MH mode particles. HGFs of MH mode particles of larger sizes (100 nm, 145 nm) started a slight decrease after about 10 am and then increased again between about the noon and late evening. Particles of this mode are supposed to be more aged than particles in the LH mode, having a substantial fraction of inorganic components such as sulfate and nitrate. However, during daytime when the photochemical activity is stronger, the MH mode particles are expected to experience condensation of different species, especially organics, which are less hygroscopic. Hence, a slightly lower HGF of these particles was observed in the afternoon than in the morning. In case of smaller particles (30 nm, 60 nm), HGFs of MH group particles appeared to decrease during the afternoon until about 8:00 pm, suggesting that these particles were not long-range transported, but rather secondary formed either locally or from nearby emissions. Moreover, Hong et al. (2015) and Cai et al. (2017) both discussed that the lifted boundary layer height may also contribute the varied HGF during daytime due to mixing the aerosol populations of diverse aging histories.

The number fractions of different-size particles in each mode are illustrated in the lower panels of Fig. 4. For larger particles (100 nm, 145 nm), MH mode particles dominated over the LH mode particles. For smaller particles (30 nm, 60 nm), the number fraction of LH mode particles decreased dramatically after 12:00 am and increased back to the same level after 6:00 pm. A similar, yet less obvious, pattern was also observed for larger particles. This feature directly suggests that small particles have a lower degree of external mixing during the afternoon compared with the rest of the day, providing further evidence that local traffic emissions may be the major sources of those LH mode particles, especially the ones of smaller sizes.

The hygroscopicity of aerosol particles is ultimately driven by the relative abundances of compounds of different water uptake ability in the particle phase. Hence, we also looked at HGFs of aerosol particles in terms of their direct composition information. Our ACSM measured the non-size resolved chemical composition of particles, which may deviate considerably from that of Aitken mode particles, but be close to that of accumulation mode particles. This requires us to choose HGF of larger particles (100 nm, 145 nm) for the analysis. In Fig. 5, the HGFs of accumulation mode particles correlate quite well with the mass fraction ratio between inorganics and organics + BC. However, the oxidation level of the organic fraction appears to exert only a slight influence on the hygroscopicity of the suburban aerosols, with R^2 values of around 0.2. Gysel et al. (2007) suggested that, compared with HGFs of pure organic particles affected strongly by their oxidation level (Duplissy et al., 2011), HGFs of mixed particles are less sensitive to the properties of uncertainties of in growth factor of less hygroscopic compounds in the aerosol phase. This feature might explain why the HGFs of our suburban aerosol were influenced to a lesser extent by the oxidation level of organic compounds than aerosol particles typically studied in smog chamber measurements or measured in a boreal forest environment (Massoli et al., 2010; Tritscher et al., 2011; Hong et al., 2015).

3.3 Comparison between polluted and clean days

In order to understand the influence of primary sources and secondary formation to the aerosol loading during different synoptic conditions (e.g., relative clean days and

polluted days), we studied the chemical characteristics and physical-chemical properties of aerosols, as well as individual air mass origins, during the two distinguished periods, respectively. Figure 6 shows the diurnal variation of the major species in particle phase during the polluted and relative clean days. Concentrations of all of the displayed species were higher during the polluted period compared with the clean days. This was particularly obvious for NO_3^-, whose concentration was almost ten times higher during the polluted days. Wind speeds shown in Fig. 1 were the lowest during the polluted period, enabling local emitted air pollutants such as from traffic and cooking to accumulate. Moreover, a substantial fraction (64%) of the air mass trajectories, shown in Fig. 7, were passing along the coastal areas in the southeast of China, which is heavily populated. These coastal air masses, together with a considerable fraction (21%) of air masses circulating within the PRD region may potentially transport significant amounts of pollutants, presumably from anthropogenic emissions, to the site. Contrary to this, air masses in the clean days were mainly from the inland areas in the north. These regions are, covered with vegetation and are less influenced by anthropogenic emissions, so air masses coming from there may promote the dilution and clearance of the local pollutants at the observational site.

During the polluted days, SO_4^{2-}, NO_3^- and organics had clear diurnal patterns. Concentrations of SO_4^{2-} and organics peaked during the late afternoon, probably due to gas phase condensation or multiphase reactions associated with high levels of SO_2 or gaseous organics after long-range transport, as discussed above. Nitrate had higher concentrations in the early morning than in the afternoon. Pathak et al. (2009) suggested that high concentration of particulate nitrate could be explained by the heterogeneous hydrolysis of N_2O_5 under high relative humidity conditions. Morino et al. (2006) concluded, using both observation and thermodynamic modeling, that lower temperatures and higher RH cause an enhanced condensation of HNO_3 to the particle phase. Fig. S1 shows that RH values were higher in the early morning than other times of the day under polluted conditions. We also looked at gaseous HNO_3 concentration, obtained from MARGA measurements and found them to be less than two times higher in polluted conditions compared with clean days. The partition of HNO_3 to the particle phase due to condensation might not be able to fully explain the one-order-of-magnitude higher nitrate concentrations in particle phase in polluted days than clean days. Hence, we speculate that the heterogeneous hydrolysis of N_2O_5 could be the alternative reason for the production of the observed high concentrations of nitrate in the early morning under polluted condition. During clean days, both inorganic and organic species have lower concentration, with no strong diurnal pattern, which indirectly indicates that the influence of the elevated boundary height on the daily variation of chemical composition was minor. The concentration of BC peaked at around rush hours, suggesting traffic emissions could be one of the major sources of BC.

Considering all examined species together, the difference in the inorganics/organic+BC ratio between early morning and late afternoon was more obvious for the polluted conditions than during the clean days (lower panels of Fig. 6). The averaged O:C ratio during the polluted days was a little bit lower than during the clean days, suggesting that the organic fraction was less oxidized during pollution episode.

The HGFs correlate much better with the contribution of different species to the mass fractions during the polluted days than during the clean days (Fig. 8). However, the oxidation level had a relatively stronger influence on the HGFs during the clean days compared with the polluted days. Taken together, these observations suggest that despite the variability in its oxidation level, the hygroscopicity of the organic aerosol fraction did not vary much during the polluted days.

3.4 Hygroscopicity-composition closure

Hygroscopic growth factors of organic compounds in the aerosol phase, HGF_{org}, range widely from about 1 to 1.3 for various ambient aerosols reported in the literature (Gysel et al., 2004; Carrico et al., 2005; Aklilu et al., 2006; Good et al., 2010; Hong et al., 2015; Chen et al., 2017). No previous data are available HGF_{org} in suburban aerosols in the PRD region during seasons of the current study. Therefore, an ensemble-mean HGF_{org} of 1.1, was determined when the sum of all residuals (RMSE, root mean square error) between the measured growth factors and corresponding ZSR predictions reached a minimum by varying HGF_{org} between 1 and 1.3.

By applying HGF_{org} of 1.1, Fig. 9 compares the ACSM-derived HGF with HTDMA-measured ones for four different sized particles, with the color code indicating the O:C ratio. It is obvious that the agreement was the best for larger particles, as ACSM measured the bulk sample that is close to the chemical information of larger particles (Hong et al., 2014; Hong et al., 2015). Yeung et al. (2014) used HGF_{org} of 1.18 in the ZSR prediction of hygroscopicity for aerosols in September 2011 at the HKUST Supersite, less than 120 km away from our measurement site, and achieved slightly better agreement between the measured and the predicted HGFs. This was mostly due to they used size-resolved chemical composition in their closure analysis.

Previous studies suggest that a single ensemble HGF_{org} approximation might not be capable of evaluating the hygroscopicity of ambient aerosols from different sources with various characteristics. Hence, the HGF_{org} approximation based on the O:C ratio was also tested and the results are given in Fig. 10 for 145 nm particles. With slightly higher R^2 and slope values of the fitting between the measurements and predictions, a new relation between the HGF_{org} and O:C of the organic fraction for suburban aerosols in PRD region was obtained as followed:

$$HGF_{org} = 0.3 \cdot O{:}C + 0.87. \quad (3)$$

Previous studies (Sjogren et al., 2008; Suda et al., 2014) suggested that the interaction between inorganic and organic materials within the particle phase might alter the hygroscopicity of organics in mixtures and speculated that these interactions might be more pronounced for inorganic dominated aerosols (Hong et al., 2015). However, no apparent impact on the hygroscopicity of organic materials from inorganic materials was observed in the current study.

According to Kuwata et al. (2012), the density of SOA is dependent on the O:C ratio of the organic fraction. When using their suggested parameterization for the density of organic material in the ACSM-derived hygroscopicity, the closure analysis did not improve. However, setting the density and the O:C-dependent growth factor for

organics both as free parameters, the closure results improved considerately and we ended up with a similar relation between the HGF of organics and their oxidation level as below but a higher density value (ρ_{org}=1.37g/cm^3) for organics (see Fig. S2):

$$HGF_{org} = 0.32 \cdot O{:}C + 0.81. \quad (4)$$

By taking into account of the variation of the O:C ratio, HGF_{org} ranged from 0.85 to 1.12 with a substantial number values below 1 by applying Eq. 4. In contrast, HGF_{org} varies between 0.92 and 1.16 when using Eq. 3 with around 80% of the data having values larger than 1. This finding implies that the approximation in Eq. 4, even with a better agreement between the measured HGF and the predicted ones, may introduce huge errors, as values of HGF_{org} are not physically correct. However, special care should also be paid to applying Eq. 3 to estimate the hygroscopic properties of organic materials, especially when the O:C ratio is low. Nevertheless, organic material at this suburban background in the Panyu site during this study exhibited quite a low hygroscopicity (averaged HGF_{org} is less than 1.1), suggesting these organics are close to be hydrophobic and could be aromatic compounds or compounds with long carbon chains or having larger molecular weight.

The interpretation of different approximation of HGF_{org} above reveals that in order to estimate accurately the properties of ambient aerosols, we might need to have precise measurements of chemistry, including the size-dependent chemical composition of the aerosols, as well as a better prediction model for HGF.

3.5 Synthetic Comparisons

A number of field studies have examined the relationship between the hygroscopicity of organic materials and their oxidation level for ambient aerosols from various representative organic aerosol sources (Chang et al., 2010; Chen et al., 2017; Duplissy et al., 2011; Hong et al., 2015a; Mei et al., 2013; Wu et al., 2013, 2016). The empirical relationship obtained from our results and these earlier studies are compared and described below and in Fig. 11. It should be noted that the results from other studies shown in Fig. 11 were obtained using the hygroscopicity parameter (κ_{org}) (the left y-axis), while HGF_{org} (the right y-axis) is given in this study, both representing a quantitative measure of the hygroscopicity of organic materials. A thorough description to derive hygroscopicity parameter κ from HTDMA-measured HGF is given in Petters & Kreidenweis (2007).

All listed studies show that the hygroscopicity of organics generally increases with an increasing organic oxidation level, with significant variance in the fitting slopes among all of the empirical relationships. For aerosols from near remote (Hong et al., 2015) or rural background (Chang et al., 2010; Wu et al., 2013) areas, covering little or no influence from anthropogenic activities, O:C exhibits a stronger impact on the water uptake ability of organic materials. This indicates that the oxidation potential from photooxidation in the atmosphere of these backgrounds is a critical factor in determining the characteristics of organic materials. Exceptionally, hygroscopicity of organics from Wu et al., (2013) exhibited a weaker dependence on O:C than those of other rural background areas (Chang et al., 2010), which could be explained by the fact that their measurement site is located in central Germany, where anthropogenic

activities could not be neglected. Similar to aerosols formed from biogenic precursors, the apparent O:C dependency on the hygroscopicity of organics is obvious for peat burning aerosols (Chen et al., 2017), mostly due to the complexity in the types of biomasses.

In the suburban or urban atmosphere of megacities in China, the hygroscopicity of organic material was almost constant, being much less sensitive towards the variation in their oxidation level. In contrast, κ_{org} of aerosols at an urban site in Pasadena, California, in US exhibited a stronger increase with an increasing O:C ratio (Mei et al., 2013). They found that the relationship of their study is in line with that obtained from HTDMA measurements of SOA formed from 1,3,5-trimethylbenzene (TMB), a surrogate for anthropogenic precursors (Duplissy et al., 2011). They also deduced that the major components in SOA from TMB photooxidation are mainly mono-acids, which are quite water soluble. The comparisons of κ_{org} or HGF_{org} as a function of O:C within these aforementioned studies suggest that the anthropogenic precursors or the photooxidation mechanisms, under the suburban/urban atmosphere in China might differ significantly from those in the urban background of West US. This may lead to distinguished characteristics of the oxidation products in SOA, probably being less water soluble, and therefore to a different relationship between κ_{org}/HGF_{org} and O:C.

Other studies have attempted to use a simplified κ_{org} of 0.1 (corresponding value of HGF_{org} as 1.2) to describe the Cloud Condensation Nuclei (CCN) -activity and to calculate the CCN concentrations for field aerosols (Wang et al., 2008; Gunthe et al., 2009). However, if either this constant or the O.C dependent hygroscopicity parameter from these local environments of previous studies for organic material were applied into the climate models for suburban/urban atmosphere in China, the CCN concentrations would probably be over-predicted as the organic material in these locations appeared to be close to hydrophobic, especially in the case from the current results (HGForg = 1~1.1, the corresponding κ_{org} = 0~0.04). This indicates that in order to accurately estimate the CCN-activity, one value of κ_{org} or HGF_{org} should not be applied to all aerosol types. Further studies in environments with aerosols of various level of oxidation are needed to determine a better parametrization for organic hygroscopicity, to be incorporated into different large-scale atmospheric models.

4. Summary and conclusions

The hygroscopic growth factor distribution obtained in the late summer of 2016 at Panyu CAWNET station in PRD region suggests that this suburban aerosol population with strong anthropogenic influence was almost always externally mixed. The diurnal variation of the HGF of the LH and MH mode particles of four sizes suggests that LH mode particles were probably from local emissions, whereas the MH mode particles had a longer aging history. During daytime, the external mixing of particles decreased due to condensation of different gaseous species on them, which was particularly obvious for Aitken mode particles. The contribution of different species with various water affinities to the particle composition determines the variation of the mean HGF in general. However, the oxidation level of organics appeared to influence the hygroscopicity of the suburban aerosols only slightly.

The stagnant meteorological conditions favored the accumulation of pollutants originating from coastal areas in the southeast China during the polluted days. During these days, the hygroscopicity of the organic aerosol fraction was estimated to vary little despite the variability of its oxidation level. The atmosphere was cleared by the air masses from the north during clean days.

ACSM-derived HGF correlated quite well with the HTDMA-measured ones for larger particles. From the closure analysis, a new relation between the hygroscopic growth factor of organics and their oxidation level was obtained, HGF_{org}= 0.3 × O:C + 0.87, for the suburban aerosols over the PRD region during the experimental periods. Clearly, a quite low hygroscopicity of organic materials, with values of HGF_{org} ranging between 1 and 1.1, was observed and it exhibited a weak dependence on the O:C ratio for the current study. At this point, we can speculate that these less-hygroscopic organic materials in the suburban/urban aerosols under the strong anthropogenic influences in China could be oxidation products from aromatics or long-chain carbons after oligomerization processes.

Large-scale models normally attempt to quantify the hygroscopicity of organic materials in a simplified way. Specifically, these climate models usually use a constant parameterization for the organic hygroscopicity, or an empirical O:C-dependent κ_{org} from previous smog chamber measurements (Massoli et al., 2009; Lambe et al., 2011) or from similar field background measurements (Mei et al., 2013). This new empirical relationship between HGF_{org} and the atomic O:C ratio under the suburban atmosphere in China is essentially relevant in reducing the uncertainties inherent to models by providing a specific hygroscopicity parameterization of organic materials to the aerosol type presented in this study. Furthermore, no generality of the relationship between the hygroscopicity and the oxygenation of the organic compounds can be used for all types of aerosols.

Acknowledgements

This work was financially supported by the Kone-Fudan Nordic Center through Kone Foundation. This research has also received funding from the National Key Project of MOST (2016YFC0201901), Natural Science Foundation of China (No. 41705099, 41575113, 4160050448 and 91644213) and the Royal Society Newton Advanced Fellowship (NA140106).

References

Adam, M., Putaud, J. P., Martins dos Santos, S., Dell'Acqua, A. and Gruening, C.: Aerosol hygroscopicity at a regional background site (Ispra) in Northern Italy, Atmos. Chem. Phys., 12(13), 5703–5717, doi:10.5194/acp-12-5703-2012, 2012.

Aklilu, Y., Mozurkewich, M., Prenni, A. J., Kreidenweis, S. M., Alfarra, M. R., Allan, J. D., Anlauf, K., Brook, J., Leaitch, W. R., Sharma, S., Boudries, H. and Worsnop, D. R.: Hygroscopicity of particles at two rural, urban influenced sites during Pacific 2001: Comparison with estimates of water uptake from particle composition, Atmos. Environ., 40(15), 2650–2661, doi:10.1016/j.atmosenv.2005.11.063, 2006.

Asmi, E., Frey, A., Virkkula, A., Ehn, M., Manninen, H. E., Timonen, H., Tolonen-Kivimäki, O., Aurela, M., Hillamo, R., and Kulmala, M.: Hygroscopicity and chemical composition of Antarctic sub-micrometre aerosol particles and observations of new particle formation, Atmos. Chem. Phys., 10, 4253–4271, doi:10.5194/acp-10-4253-2010, 2010.

Bougiatioti, A., Fountoukis, C., Kalivitis, N., Pandis, S. N., Nenes, A., Mihalopoulos, N., Fountoukis, C., Pandis, S. N. and Mihalopoulos, N.: Cloud condensation nuclei measurements in the marine boundary layer of the Eastern Mediterranean: CCN closure and droplet growth kinetics, Atmos. Chem. Phys., 9(9), 7053–7066,2009.

Cabada, J. C., Khlystov, A., Wittig, A. E., Pilinis, C., and Pandis, S. N.: Light scattering by fine particles during the Pittsburgh Air Quality Study: Measurements and modeling. *J. Geophys. Res.*, 109: D16S03, 2004.

Cai, M., Tan, H., Chan, C. K., Mochida, M., Hatakeyama, S., Kondo, Y., Schurman, M. I., Xu, H., Li, F., Shimada, K., Li, L., Deng, Y., Yai, H., Matsuki, A., Qin, Y. and Zhao, J.: Comparison of Aerosol Hygroscopcity, Volatility, and Chemical Composition between a Suburban Site in the Pearl River Delta Region and a Marine Site in Okinawa, Aerosol Air Qual. Res., 17(12), 3194–3208, doi:10.4209/aaqr.2017.01.0020, 2017.

Canagaratna, M. R., Jimenez, J. L., Kroll, J. H., Chen, Q., Kessler, S. H., Massoli, P., Hildebrandt Ruiz, L., Fortner, E., Williams, L. R., Wilson, K. R., Surratt, J. D., Donahue, N. M., Jayne, J. T. and Worsnop, D. R.: Elemental ratio measurements of organic compounds using aerosol mass spectrometry: characterization, improved calibration, and implications, Atmos. Chem. Phys., 15(1), 253–272, doi:10.5194/acp-15-253-2015, 2015.

Carrico, C. M., Kreidenweis, S. M., Malm, W. C., Day, D. E., Lee, T., Carrillo, J., McMeeking, G. R. and Collett Jr., J. L.: Hygroscopic growth behavior of a carbon-dominated aerosol in Yosemite National Park, Atmos. Environ., 39(8), 1393–1404, doi:10.1016/j.atmosenv.2004.11.029, 2005.

Chang, R. Y.-W., Slowik, J. G., Shantz, N. C., Vlasenko, A., Liggio, J., Sjostedt, S. J., Leaitch, W. R. and Abbatt, J. P. D.: The hygroscopicity parameter (κ) of ambient organic aerosol at a field site subject to biogenic and anthropogenic influences: relationship to degree of aerosol oxidation, Atmos. Chem. Phys., 10(11), 5047–5064, doi:10.5194/acp-10-5047-2010, 2010.

Chen, J., Budisulistiorini, S. H., Itoh, M., Lee, W.-C., Miyakawa, T., Komzaki, Y., Yang, L. and Kuwata, M.: Water Uptake by Fresh Indonesian Peat Burning Particles is Limited by Water Soluble Organic Matter, Atmos. Chem. Phys. Discuss., 1–35, doi:10.5194/acp-2017-136, 2017.

Cheng, Y. F., Wiedensohler, A., Eichler, H., Su, H., Gnauk, T., Brüggemann, E., Herrmann, H., Heintzenberg, J., Slanina, J. and Tuch, T.: Aerosol optical properties and related chemical apportionment at Xinken in Pearl River Delta of China, Atmos. Environ., 42(25), 6351–6372, doi:10.1016/j.atmosenv.2008.02.034, 2008.

Cheng, Y. F., Wiedensohler, A., Eichler, H., Heintzenberg, J., Tesche, M., Ansmann, A., Wendisch, M., Su, H., Althausen, D. and Herrmann, H.: Relative humidity dependence of aerosol optical properties and direct radiative forcing in the surface boundary layer at Xinken in Pearl River Delta of China: An observation based numerical study, Atmos. Environ., 42(25), 6373–6397, doi:10.1016/j.atmosenv.2008.04.009, 2008.

Cheng, Y. F., Su, H., Rose, D., Gunthe, S. S., Berghof, M., Wehner, B., Achtert, P., Nowak, A., Takegawa, N., Kondo, Y., Shiraiwa, M., Gong, Y. G., Shao, M., Hu, M., Zhu, T., Zhang, Y. H., Carmichael, G. R., Wiedensohler, A., Andreae, M. O., and Poeschl, U.: Size-resolved measurement of the mixing state of soot in the megacity Beijing, China: diurnal cycle, aging and parameterization, Atmospheric Chemistry and Physics, 12, 4477-4491, 10.5194/acp-12-4477-2012, 2012.

Cheng, Y., Zheng, G., Wei, C., Mu, Q., Zheng, B., Wang, Z., Gao, M., Zhang, Q., He, K., Carmichael, G., Poschl, U., and Su, H.: Reactive nitrogen chemistry in aerosol water as a source of sulfate during haze events in China, Science Advances, 2, 10.1126/sciadv.1601530, 2016.

Dockery, D. W., Pope, C. A., Xu, X., Spengler, J. D., Ware, J. H., Fay, M. E., Ferris Jr, B. G., and Speizer, F. E.: An association between air pollution and mortality in six US cities. *N. Engl. J. Med.*, 329(24): 1753-1759, 1993.

Duplissy, J., DeCarlo, P. F., Dommen, J., Alfarra, M. R., Metzger, A., Barmpadimos, I., Prevot, A. S. H., Weingartner, E., Tritscher, T., Gysel, M., Aiken, A. C., Jimenez, J. L., Canagaratna, M. R., Worsnop, D. R., Collins, D. R., Tomlinson, J., and Baltensperger, U.: Relating hygroscopicity and composition of organic aerosol particulate matter, Atmos. Chem. Phys., 11, 1155-1165, doi:10.5194/acp-11-1155-2011, 2011.

Eichler, H., Cheng, Y. F., Birmili, W., Nowak, A., Wiedensohler, A., Brüggemann, E., Gnauk, T., Herrmann, H., Althausen, D. and Ansmann, A.: Hygroscopic properties and extinction of aerosol particles at ambient relative humidity in South-Eastern China, Atmos. Environ., 42(25), 6321–6334, doi:10.1016/j.atmosenv.2008.05.007, 2008.

Fors, E. O., Swietlicki, E., Svenningsson, B., Kristensson, A., Frank, G. P. and Sporre, M.: Hygroscopic properties of the ambient aerosol in southern Sweden – a two year study, Atmos. Chem. Phys., 11(16), 8343–8361, doi:10.5194/acp-11-8343-2011, 2011.

Good, N., Topping, D. O., Allan, J. D., Flynn, M., Fuentes, E., Irwin, M., Williams, P. I., Coe, H., and McFiggans, G.: Consistency between parameterisations of aerosols hygroscopicity and CCN activity during the RHaMBLe discovery cruise, Atmos. Chem. Phys., 10, 3189-3203, 2010.

Gunthe, S. S., King, S. M., Rose, D., Chen, Q., Roldin, P., Farmer, D. K., Jimenez, J. L., Artaxo, P., Andreae, M. O., Martin, S. T., and Pöschl, U.: Cloud condensation nuclei in pristine tropical rainforest air of Amazonia: size-resolved measurements and modeling of atmospheric aerosol composition and CCN activity, Atmos. Chem. Phys., 9, 7551–7575, doi:10.5194/acp-9-7551- 2009, 2009.

Gunthe, S. S., Rose, D., Su, H., Garland, R. M., Achtert, P., Nowak, A., Wiedensohler, A., Kuwata, M., Takegawa, N., Kondo, Y., Hu, M., Shao, M., Zhu, T., Andreae, M. O., and Pöschl, U.: Cloud condensation nuclei (CCN) from fresh and aged air pollution in the megacity region of Beijing, Atmos. Chem. Phys., 11, 11023-11039, https://doi.org/10.5194/acp-11-11023-2011, 2011.

Gysel, M., Weingartner, E., Nyeki, S., Paulsen, D., Baltensperger, U., Galambos, I. and Kiss, G.: Hygroscopic properties of water-soluble matter and humic-like organics in atmospheric fine aerosol, Atmos. Chem. Phys, 4, 35–50, 2004.

Gysel, M., Crosier, J., Topping, D. O., Whitehead, J. D., Bower, K. N., Cubison, M. J., Williams, P. I., Flynn, M. J., McFiggans, G. B., and Coe, H.: Closure study between chemical composition and hygroscopic growth of aerosol particles during TORCH2, Atmos. Chem. Phys., 7, 6131-6144, 2007.

Hansen, A. D. A., Rosen, H. and Novakov, T.: Real-time measurement of the absorption coefficient of aerosol particles, Appl. Opt., 21(17), 3060, doi:10.1364/AO.21.003060, 1982.

Hong, J., Häkkinen, S. A. K., Paramonov, M., Äijälä, M., Hakala, J., Nieminen, T., Mikkilä, J., Prisle, N. L., Kulmala, M., Riipinen, I., Bilde, M., Kerminen, V.-M., and Petäjä, T.: Hygroscopicity, CCN and volatility properties of submicron atmospheric aerosol in a boreal forest environment during the summer of 2010, Atmos. Chem. Phys., 14, 4733-4748, doi:10.5194/acp-14-4733-2014, 2014.

Hong, J., Kim, J., Nieminen, T., Duplissy, J., Ehn, M., Äijälä, M., Hao, L. Q., Nie, W., Sarnela, N., Prisle, N. L., Kulmala, M., Virtanen, A., Petäjä, T. and Kerminen, V.-M.: Relating the hygroscopic properties of submicron aerosol to both gas- and particle-phase chemical composition in a boreal forest environment, Atmos. Chem. Phys., 15(20), 11999–12009, doi:10.5194/acp-15-11999-2015, 2015.

IPCC 2013. Climate change 2013: the physical science basis. Working Group I Contribution to the Fifth Assessment Report of the Intergovernmental Panel on Climate Change, Cambridge University Press, Cambridge, United Kingdom and New York, NY, USA.

Jiang, R., Tan, H., Tang, L., Cai, M., Yin, Y., Li, F., Liu, L., Xu, H., Chan, P. W., Deng, X. and Wu, D.: Comparison of aerosol hygroscopicity and mixing state between winter and summer seasons in Pearl River Delta region, China, Atmos. Res., 169, 160–170, doi:10.1016/j.atmosres.2015.09.031, 2016.

Kortelainen, A., Hao, L., Tiitta, P., Jaatinen, A., Miettinen, P., Kulmala, M., Smith, J. N., Laaksonen, A., Worsnop, D. R. and Virtanen, A.: Sources of particulate organic nitrates in the boreal forest in Finland, Boreal Env. Res, 22, 13–26, 2017.

Kuwata, M., Zorn, S. R. and Martin, S. T.: Using Elemental Ratios to Predict the Density of Organic Material Composed of Carbon, Hydrogen, and Oxygen, Environ. Sci. Technol., 46(2), 787–794, doi:10.1021/es202525q, 2012.

Lambe, A. T., Onasch, T. B., Massoli, P., Croasdale, D. R., Wright, J. P., Ahern, A. T., Williams, L. R., Worsnop, D. R., Brune, W. H. and Davidovits, P.: Laboratory studies of the chemical composition and cloud condensation nuclei (CCN) activity of secondary organic aerosol (SOA) and oxidized primary organic aerosol (OPOA), Atmos. Chem. Phys., 11(17), 8913–8928, doi:10.5194/acp-11-8913-2011, 2011.

Li, J., Han, Z. and Zhang, R.: Influence of aerosol hygroscopic growth parameterization on aerosol optical depth and direct radiative forcing over East Asia, Atmos. Res., 140–141, 14–27, doi:10.1016/j.atmosres.2014.01.013, 2014.

Liu, P. F., Zhao, C. S., Göbel, T., Hallbauer, E., Nowak, A., Ran, L., Xu, W. Y., Deng, Z. Z., Ma, N., Mildenberger, K., Henning, S., Stratmann, F. and Wiedensohler, A.: Hygroscopic properties of aerosol particles at high relative humidity and their diurnal variations in the North China Plain, Atmos. Chem. Phys., 11(7), 3479–3494, doi:10.5194/acp-11-3479-2011, 2011.

Liu, X. G., Li, J., Qu, Y., Han, T., Hou, L., Gu, J., Chen, C., Yang, Y., Liu, X., Yang, T., Zhang, Y., Tian, H. and Hu, M.: Formation and evolution mechanism of regional haze: a case study in the megacity Beijing, China, Atmos. Chem. Phys., 13(9), 4501–4514, doi:10.5194/acp-13-4501-2013, 2013.

Liu, X., Gu, J., Li, Y., Cheng, Y., Qu, Y., Han, T., Wang, J., Tian, H., Chen, J. and Zhang, Y.: Increase of aerosol scattering by hygroscopic growth: Observation, modeling, and implications on visibility, Atmos. Res., 132–133, 91–101, doi:10.1016/j.atmosres.2013.04.007, 2013.

Malm, W. C., Day, D. E., Kreidenweis, S. M., Collett, J. L. and Lee, T.: Humidity-dependent optical properties of fine particles during the Big Bend Regional Aerosol and Visibility Observational Study, J. Geophys. Res. Atmos., 108(D9), n/a-n/a, doi:10.1029/2002JD002998, 2003.

Massling, A., Stock, M. and Wiedensohler, A.: Diurnal, weekly, and seasonal variation of hygroscopic properties of submicrometer urban aerosol particles, Atmos. Environ., 39(21), 3911–3922, doi:10.1016/j.atmosenv.2005.03.020, 2005.

Massling, A., Stock, M., Wehner, B., Wu, Z. J., Hu, M., Brüggemann, E., Gnauk, T., Herrmann, H. and Wiedensohler, A.: Size segregated water uptake of the urban submicrometer aerosol in Beijing, Atmos. Environ., 43(8), 1578–1589, doi:10.1016/j.atmosenv.2008.06.003, 2009.

Massoli, P., Lambe, A. T., Ahern, A. T., Williams, L. R., Ehn, M., Mikkilä, J., Canagaratna, M. R., Brune, W. H., Onasch, T. B., Jayne, J. T., Petäjä, T., Kulmala, M., Laaksonen, A., Kolb, C. E., Davidovits, P., and Worsnop, D. R.: Relationship between aerosol oxidation level and hygroscopic properties of laboratory generated secondary organic aerosol (SOA) particles, Geophys. Res. Lett., 37, L24801, doi:10.1029/2010GL045258, 2010.

McMurry, P. H., Takano, H. and Anderson, G. R.: Study of the Ammonia (Gas)-Sulfuric Acid (Aerosol) Reaction Rate, Environ. Sci. Technol., 17, 347–352, 1983.

Mei, F., Hayes, P. L., Ortega, A., Taylor, J. W., Allan, J. D., Gilman, J., Kuster, W., de Gouw, J., Jimenez, J. L. and Wang, J.: Droplet activation properties of organic aerosols observed at an urban site during CalNex-LA, J. Geophys. Res. Atmos., 118(7), 2903–2917, doi:10.1002/jgrd.50285, 2013.

Meyer, N. K., Duplissy, J., Gysel, M., Metzger, A., Dommen, J., Weingartner, E., Alfarra, M. R., Prevot, A. S. H., Fletcher, C., Good, N., McFiggans, G., Jonsson, A. M., Hallquist, M., Baltensperger, U., and Ristovski, Z. D.: Analysis of the hygroscopic and volatile properties of ammonium sulphate seeded and unseeded SOA particles, Atmos. Chem. Phys., 9, 721-732, 2009.

Morino, Y., Kondo, Y., Takegawa, N., Miyazaki, Y., Kita, K., Komazaki, Y., Fukuda, M., Miyakawa, T., Moteki, N. and Worsnop, D. R.: Partitioning of HNO 3 and particulate nitrate over Tokyo: Effect of vertical mixing, J. Geophys. Res., 111(D15), D15215, doi:10.1029/2005JD006887, 2006.

Ng, N. L., Herndon, S. C., Trimborn, A., Canagaratna, M. R., Croteau, P. L., Onasch, T. B., Sueper, D., Worsnop, D. R., Zhang, Q., Sun, Y. L. and Jayne, J. T.: An Aerosol Chemical Speciation Monitor (ACSM) for Routine Monitoring of the Composition and Mass Concentrations of Ambient Aerosol, Aerosol Sci. Technol., 45(7), 780–794, doi:10.1080/02786826.2011.560211, 2011.

Park, K., Kim, J.-S. and Park, S. H.: Measurements of Hygroscopicity and Volatility of Atmospheric Ultrafine Particles during Ultrafine Particle Formation Events at Urban, Industrial, and Coastal Sites, Environ. Sci. Technol., 43(17), 6710–6716, doi:10.1021/es900398q, 2009.

Pathak, R. K., Wu, W. S. and Wang, T.: Summertime PM 2.5 ionic species in four major cities of China: nitrate formation in an ammonia-deficient atmosphere, Atmos. Chem. Phys. Atmos. Chem. Phys., 9, 1711–1722, 2009.

Rosenfeld, D., Sherwood, S., Wood, R., and Donner, L., Climate effects of aerosol-cloud interactions, science, 343, 379, doi:10.1126/science.1247490, 2014.

Reutter, P., Su, H., Trentmann, J., Simmel, M., Rose, D., Gunthe, S. S., Wernli, H., Andreae, M. O., and Pöschl, U.: Aerosol- and updraft-limited regimes of cloud droplet formation: influence of particle number, size and hygroscopicity on the activation of cloud condensation nuclei (CCN), Atmos. Chem. Phys., 9, 7067-7080, https://doi.org/10.5194/acp-9-7067-2009, 2009.

Schmale, J., D. Shindell, E. von Schneidemesser, I. Chabay, and M. G. Lawrence, Air pollution: Clean up our skies, Nature, 515, 335–337, doi:10.1038/515335a, 2014.

Seinfeld, J. H. and Pandis, S. N.: Atmospheric chemistry and physics: from air pollution to climate change. John Wiley & Sons, Inc., New York, 2016.

Sjogren, S., Gysel, M., Weingartner, E., Alfarra, M. R., Duplissy, J., Cozic, J., Crosier, J., Coe, H., and Baltensperger, U.: Hygroscopicity of the submicrometer aerosol at the high-alpine site Jungfraujoch, 3580 m a.s.l., Switzerland, Atmos. Chem. Phys., 8, 5715-5729, 2008.

Stokes, R. H. and Robinson, R. A.: Interactions in aqueous nonelectrolyte solutions. I. Solute-solvent equilibria, J. Phys. Chem., 70, 2126–2130, 1966.

Stolzenburg, M. R.: An Ultrafine Aerosol Size Distribution Measuring System. Ph.D. Thesis, Mechanical Engineering Department, University of Minnesota, Minneapolis,1988.

Stolzenburg, M. R. and McMurry, P. H.: Equations Governing Single and Tandem DMA Configurations and a New Lognormal Approximation to the Transfer Function, Aerosol Sci. Technol., 42(6), 421–432, doi:10.1080/02786820802157823, 2008.

Su, H., Rose, D., Cheng, Y., Gunthe, S., Massling, A., Stock, M., Wiedensohler, A., Andreae, M., and Poschl, U.: Hygroscopicity distribution concept for measurement data analysis and modeling of aerosol particle mixing state with regard to hygroscopic growth and CCN activation, Atmospheric Chemistry and Physics, 10, 7489-7503, 10.5194/acp-10-7489-2010, 2010.

Suda, S. R., Petters, M. D., Yeh, G. K., Strollo, C., Matsunaga, A., Faulhaber, A., Ziemann, P. J., Prenni, A. J., Carrico, C. M., Sullivan, R. C., and Kreidenweis, S. M.: Influence of functional groups on organic aerosol cloud condensation nucleus activity, Environ. Sci. Technol., 48, 10182-10190, doi:10.1021/es502147y, 2014.

Swietlicki, E., Hansson, H. C., Hämeri, K., Svenningsson, B., Massling, A., McFiggans, G., McMurry, P. H., Petäjä, T., Tunved, P., Gysel, M., Topping, D., Weingartner, E., Baltensperger, U., Rissler, J., Wiedensohler, A., and Kulmala, M.: Hygroscopic properties of submicrometer atmospheric aerosol particles measured with H-TDMA instruments in various environments – a review, Tellus., 60B, 432-469, 2008.

Tie, X., Wu, D., and Brasseur, G.: Lung cancer mortality and exposure to atmospheric aerosol particles in Guangzhou, China, Atmos. Environ., 43, 2375–2377, 2009.

Tan, H., Liu, L., Fan, S., Li, F., Yin, Y., Cai, M. and Chan, P. W.: Aerosol optical properties and mixing state of black carbon in the Pearl River Delta, China, Atmos. Environ., 131, 196–208, doi:10.1016/j.atmosenv.2016.02.003, 2016.

Tang, I. N.: Chemical and size effects of hygroscopic aerosols on light scattering coefficients, J. Geophys. Res. Atmos., 101(D14), 19245–19250, doi:10.1029/96JD03003, 1996.

Tritscher, T., Jurányi, Z., Martin, M., Chirico, R., Gysel, M., Heringa, M. F., DeCarlo, P. F., Sierau, B., Prévôt, A. S. H., Weingartner, E. and Baltensperger, U.: Changes of hygroscopicity and morphology during ageing of diesel soot, Environ. Res. Lett., 6(3), 34026, doi:10.1088/1748-9326/6/3/034026, 2011.

Tritscher, T., Dommen, J., Decarlo, P. F., Gysel, M., Barmet, P. B., Praplan, A. P., Weingartner, E., Prévôt, A. S. H., Riipinen, I., Donahue, N. M. and Baltensperger, U.: Volatility and hygroscopicity of aging secondary organic aerosol in a smog chamber, Atmos. Chem. Phys. Atmos. Chem. Phys., 11, 11477–11496, doi:10.5194/acp-11-11477-2011, 2011.

Wang, J., Lee, Y.-N., Daum, P. H., Jayne, J., and Alexander, M. L.: Effects of aerosol organics on cloud condensation nucleus (CCN) concentration and first indirect aerosol effect, Atmos. Chem. Phys., 8, 6325–6339, doi:10.5194/acp-8-6325-2008, 2008.

Wang J., Zhao B., Wang S., Yang F., Xing J., Morawska L., Ding A., Kulmala M., Kerminen V.-M., Kujansuu J., Wang Z., Ding D., Zhang X., Wang H., Tian M., Petäjä T., Jiang J. and Hao J.: Particulate matter pollution over China and the effects of control policies. Sci. Total Environ. 584-585, 426-447, 2017.

Whitehead, J. D., Irwin, M., Allan, J. D., Good, N. and McFiggans, G.: A meta-analysis of particle water uptake reconciliation studies, Atmos. Chem. Phys., 14(21), 11833–11841, doi:10.5194/acp-14-11833-2014, 2014.

Wu, D., Mao, J. T., Deng, X. J., Tie, X. X., Zhang, Y. H., Zeng, L. M., Li, F., Tan, H. B., Bi, X. Y., Huang, X. Y., Chen, J. and Deng, T.: Black carbon aerosols and their radiative properties in the Pearl River Delta region, Sci. China, Ser. D Earth Sci., 52(8), 1152–1163, doi:10.1007/s11430-009-0115-y, 2009.

Wu, Z. J., Poulain, L., Henning, S., Dieckmann, K., Birmili, W., Merkel, M., van Pinxteren, D., Spindler, G., Müller, K., Stratmann, F., Herrmann, H. and Wiedensohler, A.: Relating particle hygroscopicity and CCN activity to chemical composition during the HCCT-2010 field campaign, Atmos. Chem. Phys., 13(16), 7983–7996, doi:10.5194/acp-13-7983-2013, 2013.

Wu, Z. J., Zheng, J., Shang, D. J., Du, Z. F., Wu, Y. S., Zeng, L. M., Wiedensohler, A., Hu, M. and Wu, Z.: Particle hygroscopicity and its link to chemical composition in the urban atmosphere of Beijing, China, during summertime, Atmos. Chem. Phys, 16, 1123–1138, doi:10.5194/acp-16-1123-2016, 2016.

Ye, X., Tang, C., Yin, Z., Chen, J., Ma, Z., Kong, L., Yang, X., Gao, W. and Geng, F.: Hygroscopic growth of urban aerosol particles during the 2009 Mirage-Shanghai Campaign, Atmos. Environ., 64, 263–269, doi:10.1016/j.atmosenv.2012.09.064, 2013.
Yeung, M. C., Lee, B. P., Li, Y. J. and Chan, C. K.: Simultaneous HTDMA and HR-ToF-AMS measurements at the HKUST supersite in Hong Kong in 2011, J. Geophys. Res., 119(16), 9864–9883, doi:10.1002/2013JD021146, 2014.

Zdanovskii, B.: Novyi metod rascheta rastvorimostei elektrolitov v mnogokomponentnykh sistema, Zh. Fiz. Khim+., 22, 1478–1485, 1486–1495, 1948.

Zhang, R., Khalizov, A. F., Pagels, J., Zhang, D., Xue, H. and McMurry, P. H.: Variability in morphology, hygroscopicity, and optical properties of soot aerosols during atmospheric processing., Proc. Natl. Acad. Sci. U. S. A., 105(30), 10291–6, doi:10.1073/pnas.0804860105, 2008.

Zhang, Q., Jimenez, J., Canagaratna, M., Ulbrich, I., Ng, N., Worsnop, D., and Sun, Y.: Understanding atmospheric organic aerosols via factor analysis of aerosol mass spectrometry: a re- view, Anal. Bioanal. Chem., 401, 3045–3067, 2011.

Zheng, G. J., Duan, F. K., Su, H., Ma, Y. L., Cheng, Y., Zheng, B., Zhang, Q., Huang, T., Kimoto, T., Chang, D., Poeschl, U., Cheng, Y. F., and He, K. B.: Exploring the severe winter haze in Beijing: the impact of synoptic weather, regional transport and heterogeneous reactions, Atmospheric Chemistry and Physics, 15, 2969-2983, 10.5194/acp-15-2969-2015, 2015.

Zieger, P., Väisänen, O., Corbin, J. C., Partridge, D. G., Bastelberger, S., Mousavi-Fard, M., Rosati, B., Gysel, M., Krieger, U. K., Leck, C., Nenes, A., Riipinen, I., Virtanen, A. and Salter, M. E.: Revising the hygroscopicity of inorganic sea salt particles, Nat. Commun., 8, 15883, doi:10.1038/ncomms15883, 2017.

Table 1. Hygroscopic growth factors of all compounds and their individual density used in the ZSR calculation.

Compounds	Density (kg m^{-3})	HGF (90%)	
		Aitken Mode (30 nm, 60 nm)	Accumulation mode (100 nm, 145 nm)
$(NH_4)_2SO_4$[a]	1769	1.66	1.70
NH_4HSO_4	1780	1.74	1.78
NH_4NO_3	1720	1.74	1.80
H_2SO_4	1830	2.02	2.05
Organics	1250[b]	1.0-1.3[c]	

a: hygroscopic growth factor and density values of all inorganic was chosen from Gysel et al. (2007)
b: density of organic materials was chosen from Yeung et al. (2014)
c: hygroscopic growth factor for organic materials were varied from 1 to 1.3 according to literature values (Gysel et al., 2004; Carrico et al., 2005; Aklilu et al., 2006; Good et al., 2010; Hong et al., 2015; Chen et al., 2017)

Atmos. Chem. Phys. Discuss., https://doi.org/10.5194/acp-2018-77
Manuscript under review for journal Atmos. Chem. Phys.
Discussion started: 15 February 2018

970

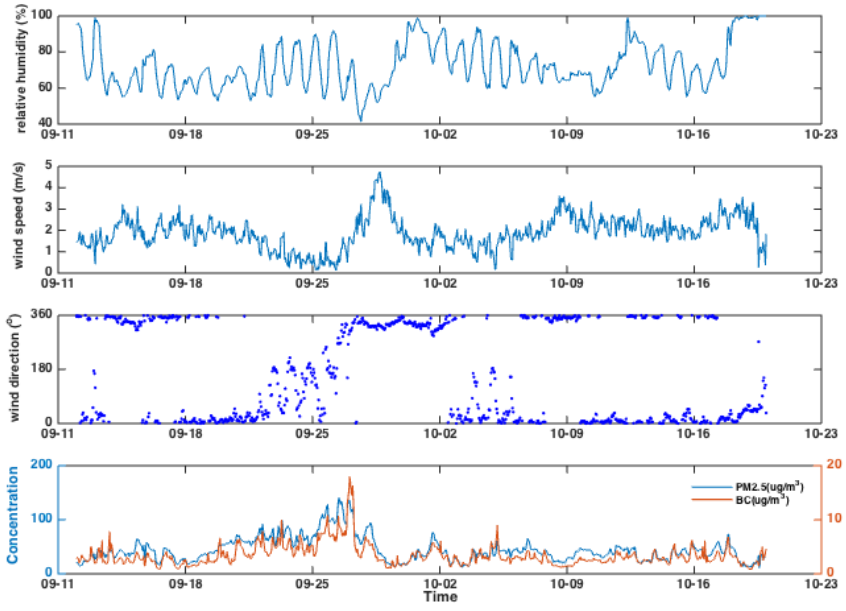

975

Figure 1. Time series for relative humidity, wind speeds, wind directions and concentrations of $PM_{2.5}$ as well as BC concentration (bottom panel).

980

Atmos. Chem. Phys. Discuss., https://doi.org/10.5194/acp-2018-77
Manuscript under review for journal Atmos. Chem. Phys.
Discussion started: 15 February 2018

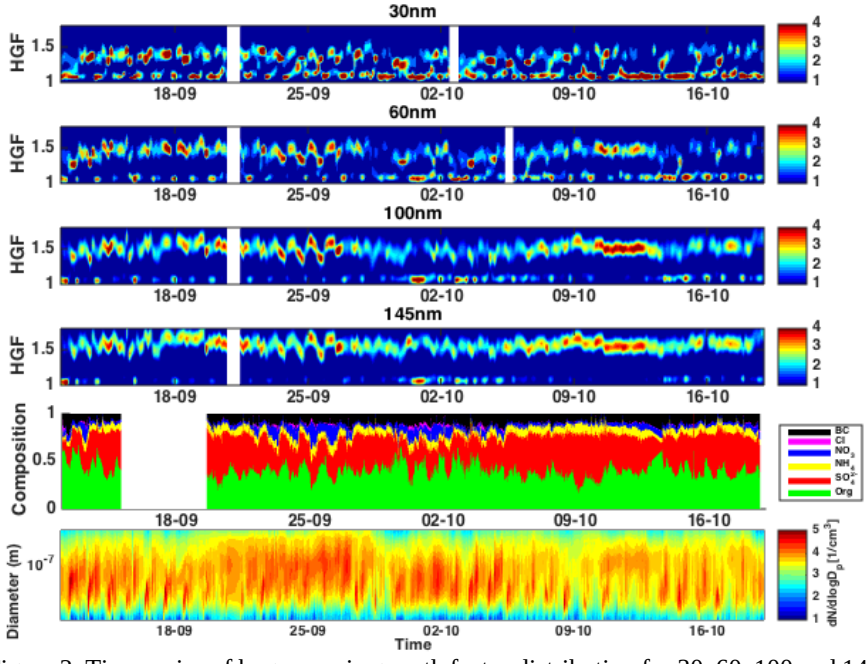

Figure 2. Time series of hygroscopic growth factor distribution for 30, 60, 100 and 145 nm particles using HTDMA in the upper four panels with the color code indicating probability density. Time series of mass fractions of chemical species in submicron particles and particle number size distribution within 10-1000 nm using ACSM and DMPS, respectively in the lower two panels.

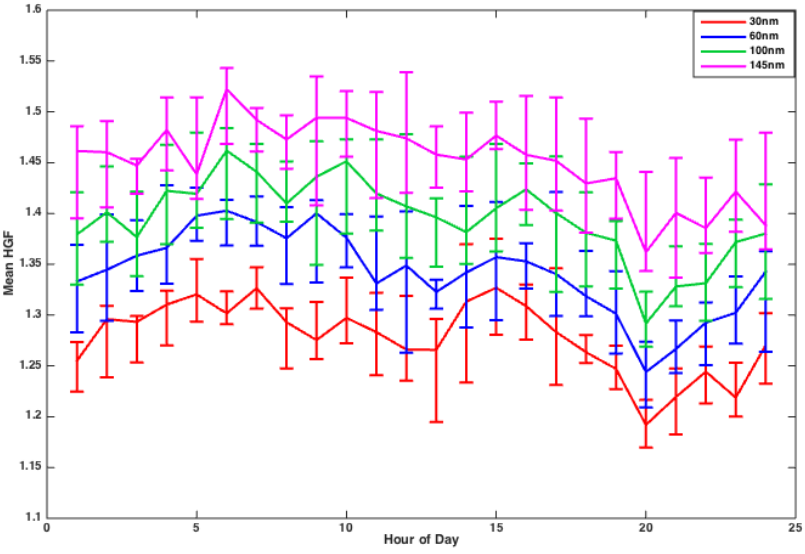

Figure 3. Diurnal variation of the mean hygroscopic growth factor of 30, 60, 100 and 145 nm particles during this study.

Atmos. Chem. Phys. Discuss., https://doi.org/10.5194/acp-2018-77
Manuscript under review for journal Atmos. Chem. Phys.
Discussion started: 15 February 2018

Atmospheric Chemistry and Physics Discussions

1045

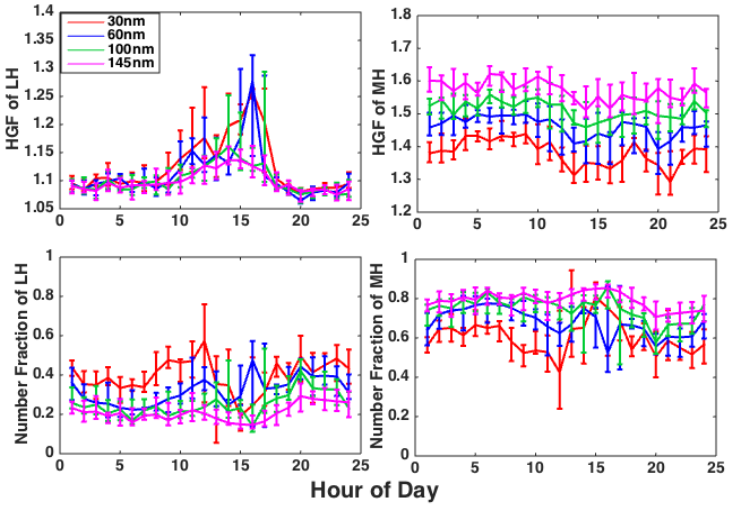

Figure 4. Diurnal variation of the HGF of LH and MH mode particles and their respective number fractions.

1050

1055

1060

1065

1070

1075

Atmos. Chem. Phys. Discuss., https://doi.org/10.5194/acp-2018-77
Manuscript under review for journal Atmos. Chem. Phys.
Discussion started: 15 February 2018

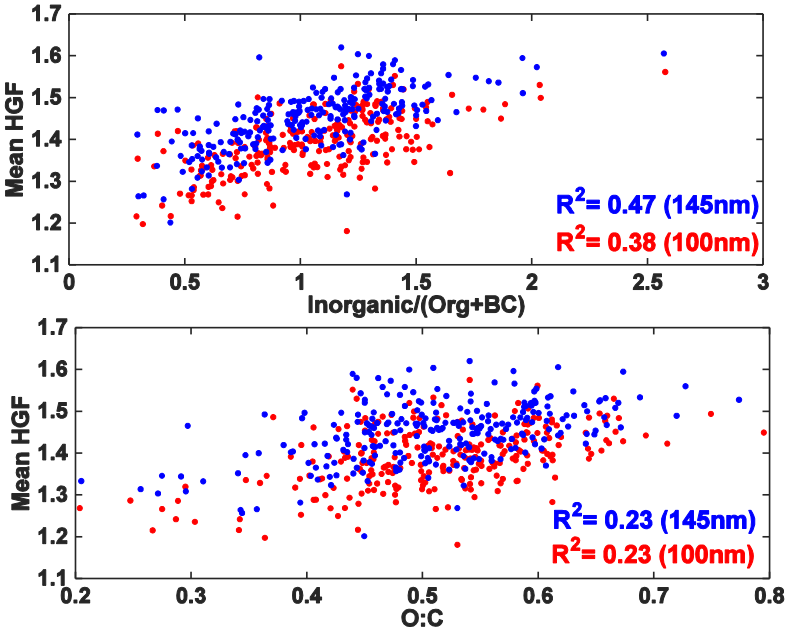

Figure 5. The correlation between the mean HGF of accumulation mode particles (100 nm, 145 nm in size) and the contribution of different species in the particle phase as well as the O:C of the organic materials.

Atmos. Chem. Phys. Discuss., https://doi.org/10.5194/acp-2018-77
Manuscript under review for journal Atmos. Chem. Phys.
Discussion started: 15 February 2018

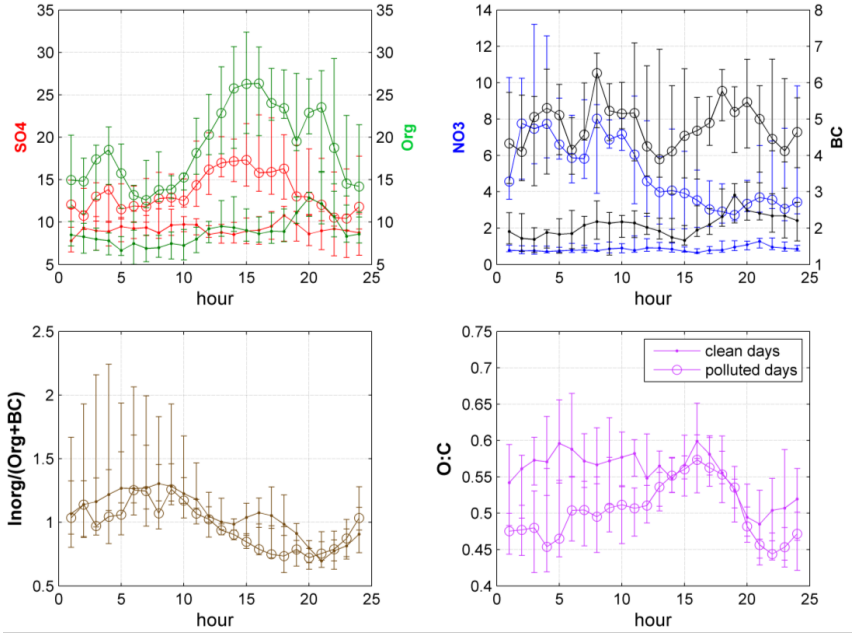

Figure 6. Diurnal variation of mass concentration of SO_4^{2-}, organics, NO_3^-, BC in particle phase, the O:C ratio of organics and their relative contribution in particle phase composition during clean days and polluted days, respectively.

Atmos. Chem. Phys. Discuss., https://doi.org/10.5194/acp-2018-77
Manuscript under review for journal Atmos. Chem. Phys.
Discussion started: 15 February 2018

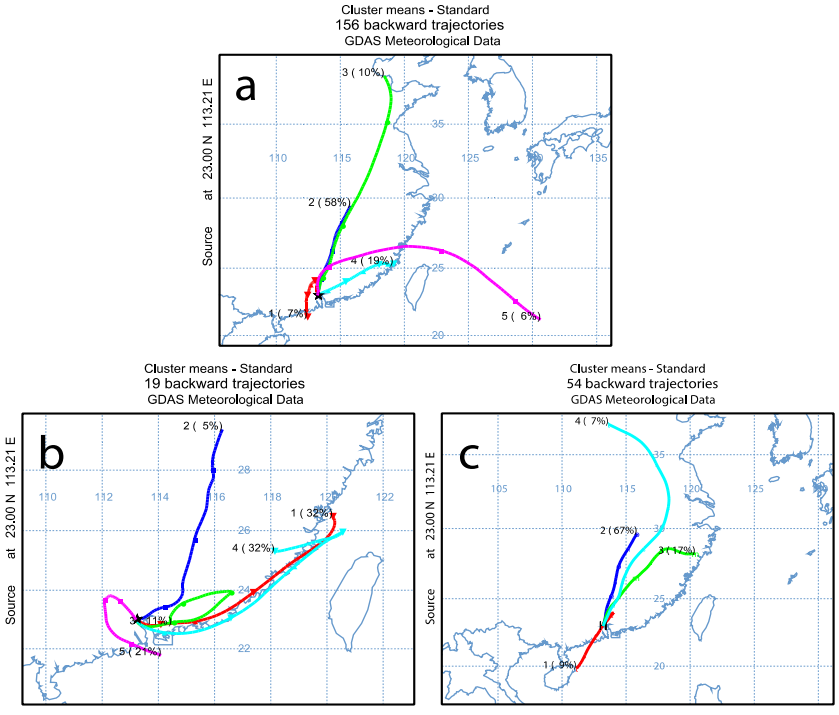

Figure 7. The major clusters for the 72-hour backward trajectory simulation for air masses arriving at the CAWNET Panyu site. The upper panel shows the results throughout the whole observational period, while the lower panel on the left side shows the one during polluted days and the one on the right-hand side is for clean days.

Atmos. Chem. Phys. Discuss., https://doi.org/10.5194/acp-2018-77
Manuscript under review for journal Atmos. Chem. Phys.
Discussion started: 15 February 2018

Atmospheric Chemistry and Physics Discussions

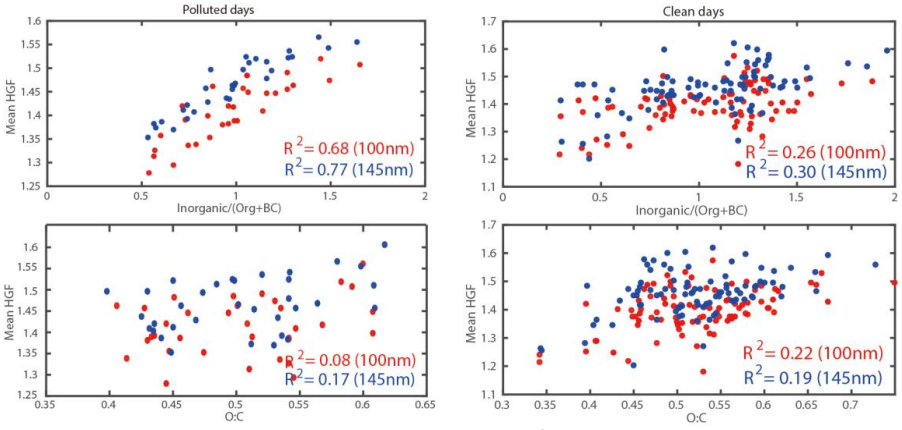

Figure 8. The correlation between the mean HGFs of accumulation mode particles (100 nm, 145 nm in size) and the contribution of different species in the particle phase as well as the O:C of the organic materials during polluted days and clean days, respectively.

Atmos. Chem. Phys. Discuss., https://doi.org/10.5194/acp-2018-77
Manuscript under review for journal Atmos. Chem. Phys.
Discussion started: 15 February 2018

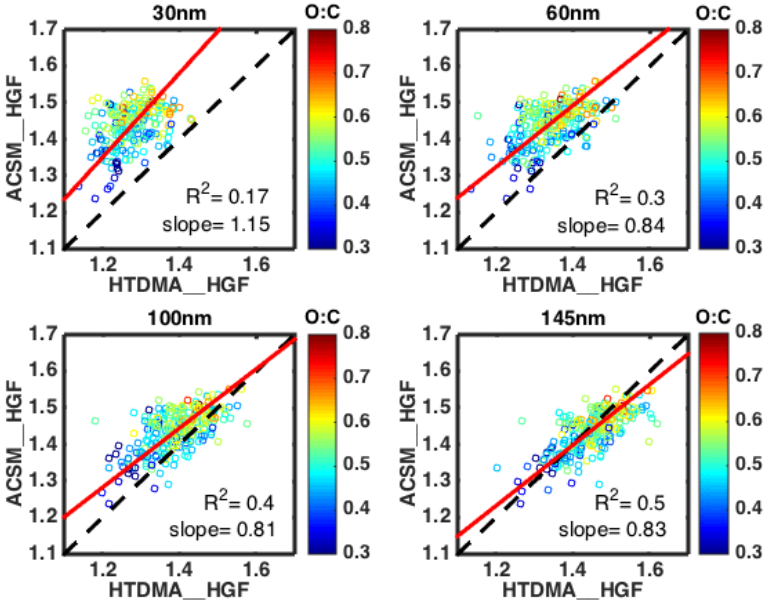

Figure 9. Closure study between the HTDMA-measured HGFs and the ACSM-derived HGFs. The dash lines indicate the 1:1 line, while the red ones are the lines fitted to the data points. The color bar indicates the O:C ratio of the organic aerosol fraction.

Atmos. Chem. Phys. Discuss., https://doi.org/10.5194/acp-2018-77
Manuscript under review for journal Atmos. Chem. Phys.
Discussion started: 15 February 2018

Atmospheric Chemistry and Physics Discussions

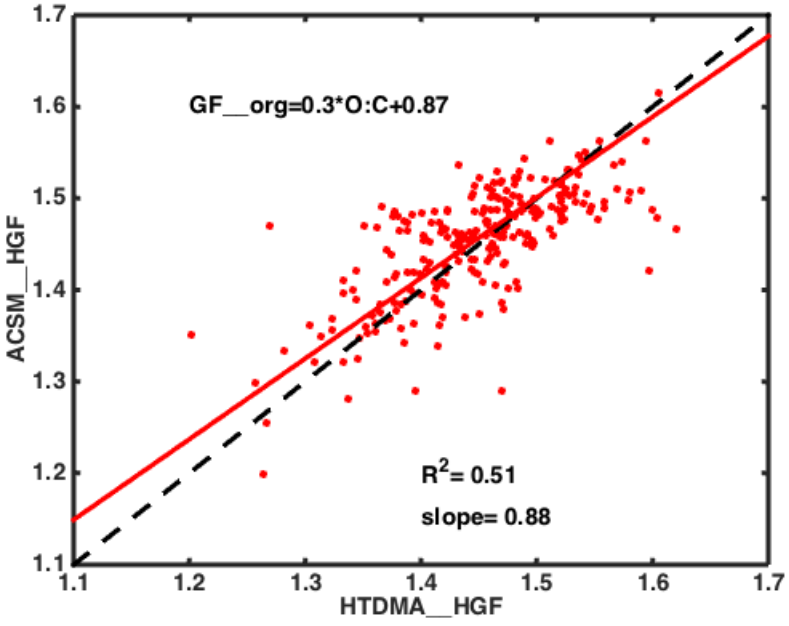

1185 Figure 10. Closure analysis with the best fitting between the measured HGFs and the ACSM-derived ones using the O:C-dependent HGF_{org}. The equation is the achieved approximation for HGF_{org} as a function of the O:C of organic aerosol fraction.

1190

1195

1200

1205

1210

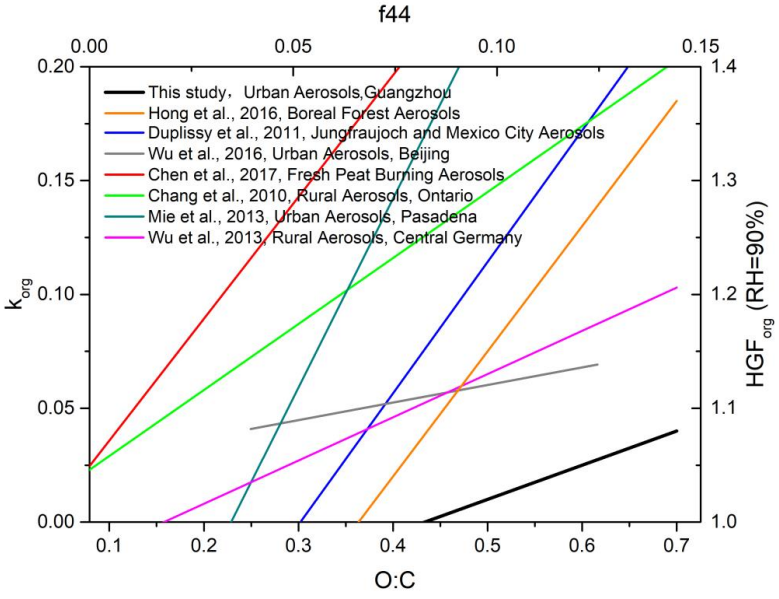

Figure 11: Comparison with earlier studies on the hygroscopicity of organic material with atomic O:C ratio (or *f44* from chemical composition data) obtained from different environmental background areas. Other studies were using derived κ_{org}, while this study is using HGF_{org} for the hygroscopicity of organic material.